Extending the field of view of imaging behind turbid media beyond the memory effect

SUBAS SCHEIBLER, MIRCO ACKERMANN, ARCHANA MALAVALLI AND CHRISTOF M. AEGERTER

Physik-Institut, University of Zurich, Winterthurerstrasse 190
8057 Zurich, Switzerland
aegerter@physik.uzh.ch

Abstract: Fluorescent imaging behind turbid layers has recently become available using several different methods based on speckle correlations. The limited range of these speckle correlations embodied in the memory effect however leads to a severe limitation of the field of view of these imaging techniques. Here, we present a method based on iterative scanning and re-focusing using wavefront shaping, such that neighbouring regions to the field of view of the memory effect can be imaged. This allows for an extension of the field of view of scattered light fluorescence microscopy far beyond the limits given by the memory effect. With this addition, applications in real life turbid media become possible, which can also be extended to dynamic media using possible improvements in speed of focusing.

1. Introduction

Scattering and diffusion of light are large limitations for optical imaging.
Recent progress has enabled imaging even in highly turbid media, where multiply scattered light is controlled, either in transmission [1–7], or in reflection [8, 9]. These techniques are based on the adjustment of the phase of the illuminating light in response to the turbid medium, such that enhanced constructive interference behind a turbid layer is possible leading to a focus even behind an intransparent layer of white paint [10]. The imaging information can then be obtained by utilizing the phase information retained over a small angle by the optical memory effect [1, 11, 12]. One main obstacle by using this technique at the moment is that the field of view is therefore limited by the angular range of the memory effect, which decreases with the thickness of the turbid layer. Here, we propose and experimentally implement a method that extends the work of [3] and can overcome the limitation set by the optical memory effect, thus allowing the possibility of wide field imaging by iteratively adjusting the shaped wavefront according to the information obtained from within the range of the memory effect. This correspondingly has a large impact on wide ranging fields of imaging, notably in biological systems, where in-vivo imaging of structures is often limited by turbid layers of materials.

2. Samples and setup

As a turbid sample, we covered one side of a glass slide (thickness: 1 mm) with Zinc Oxide pigment. The thickness of the paint layer was approximately 11 μm corresponding to more than 11 mean free paths. Thus, the layer is completely intransparent. On the other side of the glass slide we attached fluorescent beads (*FluoSpheres*^{TM}) from Thermo Fisher Scientific with a diameter of 4 μm. These beads have their maximum of excitation at 505 nm and the peak of the emission at 515 nm. The beads are applied by first diluting them in deionized water or in ethanol. A droplet (10 μl to 230 μl) was spread uniformly by putting a second glass slide on top. This last step is important in order to avoid clusters of beads on the sample.

In the optical setup (see Fig. 1) we have a laser beam as a light source (Spectra Physics Cyan 40 mW, 488 nm). The light first passes through a beam expander and is then reflected onto a spatial light modulator display (Holoeye HEO 1080 P). The light coming from the SLM is sent with help of two mirrors onto an objective (Zeiss A-Plan 40x/0.25), which images the SLM onto the front side of the turbid medium. The optimization of the incoming wavefront is carried out by the computer controlled SLM [13]. The scanning in the x-y plane is done as well with the SLM by adding a gradient which leads to a linear phase shift. A second microscope objective (Leitz NPL 40x/0.70) images the back surface of the sample on a CCD camera (ATV Stingray F-145B) serving as the detector. In order to detect only the fluorescent light a Semrock Brightline filter is mounted in front of the CCD camera.

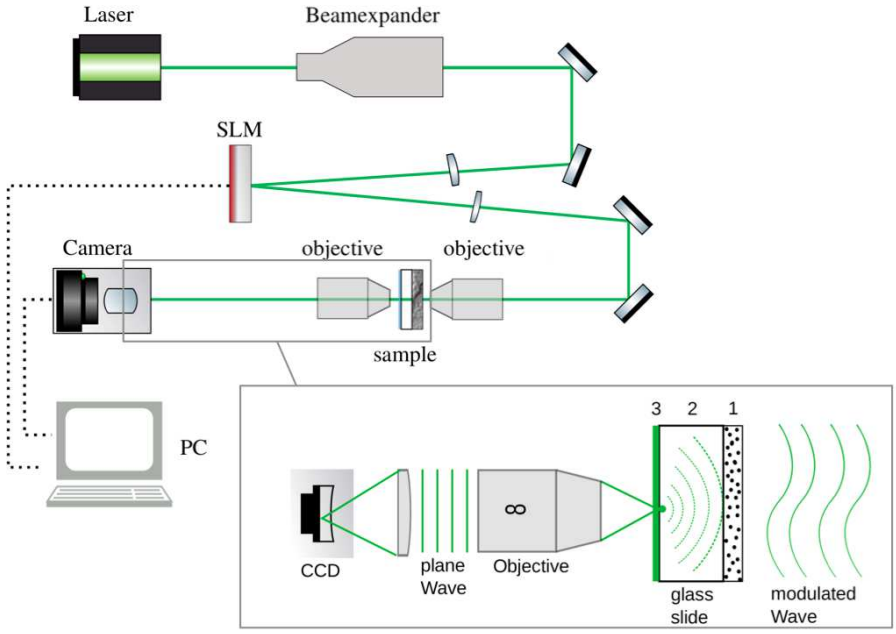

Fig. 1. Schematic drawing of the experimental setup. The laser beam which servers as a light source is first expanded such that the diameter of its cross-section is as big as the SLM display. The SLM is used to optimize the incoming wavefront to a focus behind the turbid layer and as well for scanning in the x-y plane. The signal behind the turbid layer is detected by the CCD camera.
The bottom part of the figure, schematically shows the process of focusing and sending the signal to the CCD camera in more detail. From right to left we see the modulated and optimized wave from the SLM entering the turbid medium (**1**). In a second part the wave propagates through the glass slide (**2**) and creates a focus on the layer of the fluorescent beads (**3**). The now excited fluorescent bead is emitting its signal through an infinity corrected objective (Leitz NPL 40x/0.70) finally to the CCD camera.

3. Theoretical description

As introduced in [1], scanning of the focus due to wavefront shaping and hence imaging of fluorescent beads is possible due to the optical memory effect [11, 12]. In addition, [3] have shown that such an imaging of fluorescent beads is also possible without visual access using iterative focusing directly on the fluorescence response of the beads themselves as a feedback signals. The information after a spatial variation in the phase and amplitude of an incident wave

is preserved to a certain extent during its transmission even through a highly random, completely turbid multiple scattering medium. This correlation of the phase allows for the addition of phase patterns that shift the interferometric focus in the $x-y$ plane [1], as well as in the z-direction [2]. For a scan in the $x-y$ plane, we can shift the focal position by a distance $\Delta r = a\Delta\theta$ where a is the distance from the turbid layer to the focal plane and $\Delta\theta$ corresponds to angular range of the memory effect. Due to the memory effect, while scanning, we retain a focus up to an angle of $\Delta\theta_{\max} = \frac{\lambda}{2\cdot\pi\cdot L}$ [1, 11, 12] with λ being the wave-length of the illuminating light and L the thickness of the turbid layer.

In the present experiment we obtain a range due to the memory effect of $\Delta r_{\max} = 7$ μm using $\lambda = 488$ nm and $L = 11$ μm. This distance was verified experimentally by shifting the focal point by adding a gradient on the SLM, as shown in Fig. 2.

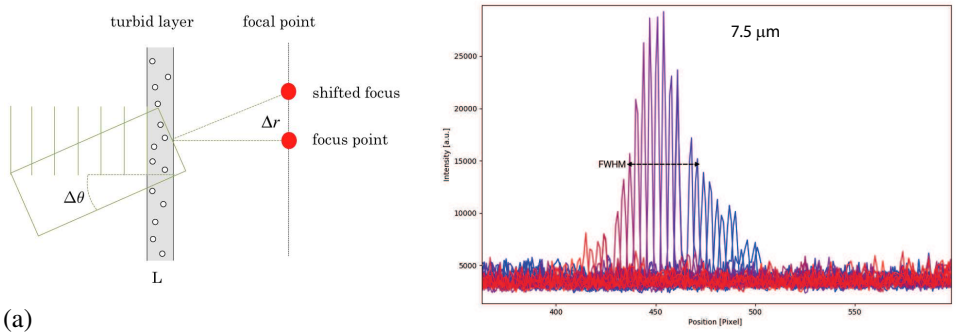

(a) (b)

Fig. 2. Schematically we see in figure (a) the geometry of scanning in the x-y plane by tilting the laser beam. The change in angle, i.e. $\Delta\theta$, is limited by the memory effect range. In figure (b) we see the intensity of many individual scanned foci as a function of its position. Furthermore the full width half max (FWHM) is indicated in the figure. This width is determined by the angular range of the optical memory effect, i.e. $\frac{a\lambda}{2\pi L}$. The resolution of the focus corresponds to the width of one peak under a colored curve. The memory effect range is the range where we still detect a signal from the focus i.e. where we measure an intensity. The maximal scan range in the positive x-direction is from the highest peak, which is the origin position of the focus (pixel number 450), to the right end (pixel number 500), where the signal is completely lost. This scan range is about 50 pixels which corresponds to 7.5 μm. The overall memory effect range can thus be quantified by the FWHM of approximately 7.5 μm.

4. Experimental results

As in [3], we use the fluorescence of the beads as feedback signal for the optimization process in the wavefront shaping in order to create the focus behind the turbid layer that is subsequently used for scanning. A direct image of these beads, each a diameter of 4 μm, can be seen in figure 3. Panels a) through c) show the transmitted fluorescence during the focusing process, where the total signal of the fluorescence is maximized in the optimization process. The algorithm segments the SLM into smaller parts in every step such that more segments contribute to the focus. The intensity of the focus increases with the number of segments. In figure c) we end with a bright focus 5 times more intense than in the beginning.

In a second step, after focusing, we scan in the area of the memory effect range in order to detect additional fluorescent beads, where the scanning is achieved by the addition of a phase gradient

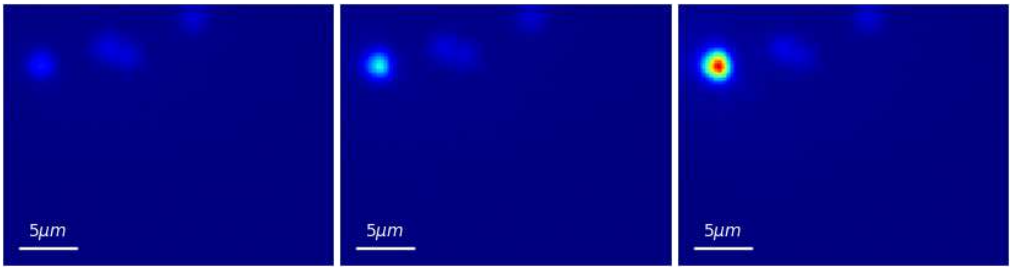

(a) (b) (c)

Fig. 3. Fluorescent signal of beads behind a turbid layer consisting of white paint during optimization of the wavefront. a) initial state, c) focusing on one of the fluorescent beads.

in the x- and y-direction respectively to the SLM and the total fluorescent signal is recorded for each position of the scan. This results in an image of the surrounding of the initial focus, shown in figure 4. Each pixel on both images corresponds to the average intensity of the CCD Camera after one scanning step. Therefore the optimized focus (i.e. the bead where we focused on) lies in the center of both images. The other high intensity areas show the position of other fluorescent beads within the field of view. In this example we choose 40 scanning steps in the x- and 40 scanning steps in the y-direction and a scanning distance of $\Delta r = +/-6\mu m$. Obviously choosing more scanning steps for the same scanning distance leads to a higher pixel density in the final image. Furthermore we implemented a threshold to choose the next closest fluorescent bead. When the algorithm found the next closest bead it loaded the corresponding phase mask to the SLM and started the optimization process anew with this starting configuration. This means that the feedback signal will be dominated by the fluorescence of this newly illuminated, neighbouring bead, such that the optimization process will lead to a focus centred on this bead.

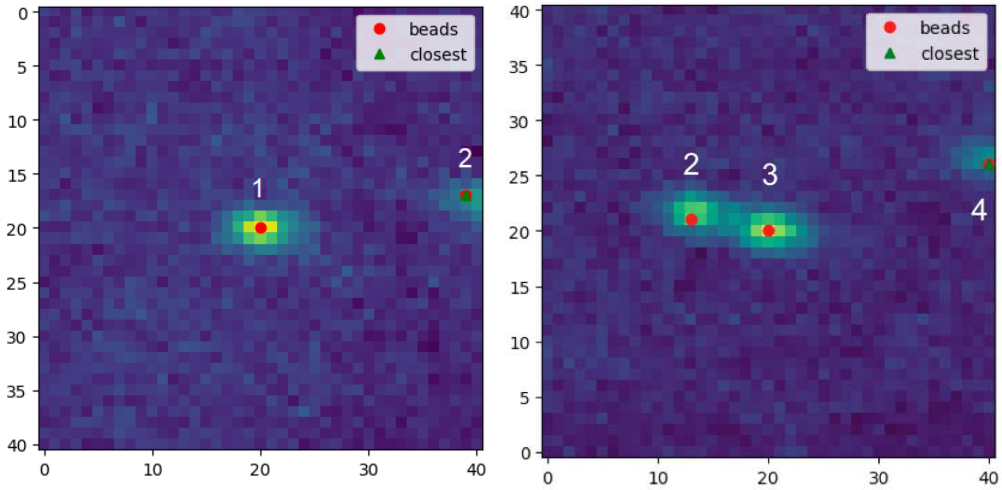

(a) (b)

Fig. 4. In this figure we see the result of the scanning and detecting process. After we optimized and focused on a bead we scanned through the sample by adding a gradient on the SLM and detecting fluorescent beads lying in that range. The numbers **1,2,3,4** are labeling the fluorescent beads and the resulting sequentially scanning process.

After creating this new focus on a bead within the field of view of the initial bead, but different

from it, we scan the range of the memory effect of this new bead, thus extending the field of view. In this manner, through iterative scanning and refocusing on fluorescent beads we are able to image far outside of the memory effect range of the starting point, with a field of view of approximately 20 μm. This final result is illustrated in figure 5, where the position of the focus can be seen to be displaced from the initial focus by several widths of the range of the memory effect. Combining the scans of these iterated foci, such as those shown in Fig. 4, a fluorescent image of the scene behind the turbid layer can thus be reconstructed with a large field of view and without direct optical access to the sample.

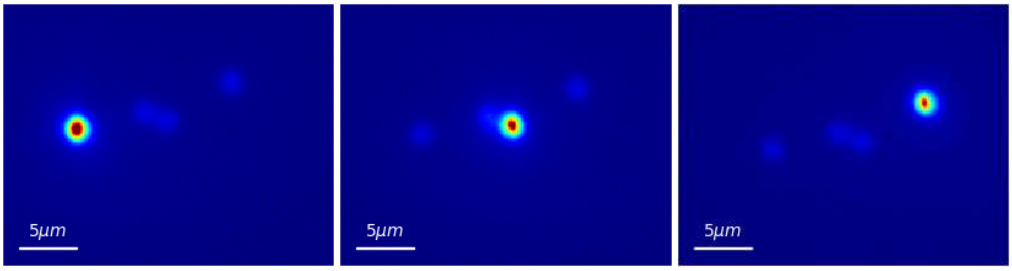

(a) (b) (c)

Fig. 5. Iterated foci after sequential scanning, detecting and refocusing on the three fluorescent beads separated further than the range of the memory effect. Panels a) through c) show the direct image of fluorescent beads after sequentially scanning through all the beads and refocusing after successive iterations on three beads.

5. Conclusion

In this work, we have presented and experimentally implemented a method with which to overcome the limited field of view of scattered light fluorescence microscopy due to the limited range of the optical memory effect [1]. We have created an algorithm, which is able to adjust the shaped wavefront according to the information obtained from the total fluorescence, thus focusing onto a bead that is not pre-determined from the outside and which thus does not need direct optical access to the sample [3]. This is extended by sequentially focusing to such an extent that the field-of-view is largely enhanced (tripled in Fig. 5) relative to the method used in [3]. More precisely, we focused on fluorescent structures behind turbid media and scanned sequentially, by detecting and refocusing on fluorescent beads laying next to each other, to such an extent that the field of view was larger than the optical memory effect range from the first focused fluorescent bead. The basis of such a technique are iterative wavefront shaping on the transmitted light [10], scanning using the memory effect [1] and the use of transmitted fluorescence as a feedback signal [3]. Given that the scanning is done directly by adding phase patterns to the SLM, also three-dimensional scanning of the focus is possible [2], such that we have in effect shown the feasibility of three-dimensional imaging behind turbid layers several mean free paths thick without direct optical access.

The resolution of the obtained images is limited by the size of the interference based focus, which in turn is only limited by the wavelength of the light used. However, it is neither determined by the optical elements used in the setup nor the scattering properties of the layer in front of the structure of interest [1, 2], i.e. diffraction limited imaging is possible behind turbid layers. The main drawback of the experimental setup used in the present work lies in the temporal resolution, which is driven by the rate of change possible in the SLM used for the optimization. With the current hardware and method of optimization, it can take up to 5 minutes to create a focus, limiting applications to static turbid media i.e. where the turbid layer is stable on time-scales

longer than the focusing and scanning time. Nevertheless recent projects in the development of piezo-element based SLMs [16] make it possible to create a focus behind a turbid media in a few milli seconds, which makes applications with living tissues possible [17, 18]. However, by decreasing the time to focus we decrease the signal for detection as well. The absorption of photons in turbid media and the resulting signal loss remains a main drawback for this experiment which might be overcome by replacing the CCD with a photomultiplier.

Acknowledgments This work was supported by the Swiss National Science Foundation (SNF)

References

1. Vellekoop, I.M., Aegerter, C.M.: Scattered light fluorescence microscopy: imaging through turbid layers. Optics Letters 35,1245-1247 (2010).
2. Ghielmetti, G. & Aegerter, C.M. Scattered light fluorescence microscopy in three dimensions Abstract. Opt. Express 20, 110âĂŞ115 (2012)
3. Ghielmetti, G. & Aegerter, C.M. Direct imaging of fluorescent structures behind turbid layers. Opt. Express 22, 1981 (2014).
4. Mosk, A. P., Lagendijk, A., Lerosey, G. & Fink, M. Controlling waves in space and time for imaging and focusing in complex media. Nature Photonics (2012). doi:10.1038/nphoton.2012.88
5. S. Popoff, G. Lerosey, M. Fink, A.C. Boccara & S. Gigan, Image transmission through an opaque material, Nature Communications 1,Article No.81,(2010).
6. Katz, O., Small, E., Bromberg, Y. & Silberberg, Y. Focusing and compression of ultrashort pulses through scattering media. Nat. Photonics (2011). doi:10.1038/nphoton.2011.72
7. Bertolotti, J, van Putten, EG, Blum, C, Lagendijk, A, Vos, WL, Mosk, AP: Non-invasive imaging through opaque scattering layers. Nature 491, 232-234 (2012).
8. Fiolka, R., Si, K. & Cui, M. Complex wavefront corrections for deep tissue focusing using low coherence backscattered light. Opt. Express (2012). doi:10.1364/OE.20.016532
9. Jang, J. et al. Complex wavefront shaping for optimal depth-selective focusing in optical coherence tomography. Opt. Express (2013). doi:10.1364/OE.21.002890
10. Vellekoop, I.M. & Mosk, A.P. Focusing coherent light through opaque strongly scattering media. Opt. Lett. 32, 2309 (2007).
11. Feng, S., Kane, C., Lee, P. A. & Stone, A. D. Correlations and fluctuations of coherent wave transmission through disordered media. Phys. Rev. Lett. 61, 834âĂŞ837 (1988).
12. Freund, I., Rosenbluh, M. & Feng, S. Memory effects in propagation of optical waves through disordered media. Phys. Rev. Lett. 61, 2328âĂŞ2331 (1988).
13. I.M.Vellekoop, Feedback-based wavefront shaping, Optics Express 23(9), pp. 12189-12206 (2015).
14. Nixon, M, Katz, O, Small, E, Bromberg, Y, Friesem, AA, Silberberg, Y, Davidson, N: Real-time wavefront shaping through scattering media by all-optical feedback. Nat Photon 7, 919-924 (2013).
15. T. Chaigne, J. Gateau, O. Katz, E. Bossy, and S. Gigan, Light focusing and two-dimensional imaging through scattering media using the photoacoustic transmission matrix with an ultrasound array, Optics Letters Vol. 39, Issue 9 (2014).
16. Blochet, B., Bourdieu, L. & Gigan, S. Focusing light through dynamical samples using fast continuous wavefront optimization. Opt. Lett. (2017). doi:10.1364/OL.42.004994
17. Edrei, E, Scarcelli, G: Optical imaging through dynamic turbid media using the Fourier-domain shower-curtain effect. Optica, 3, 71-74 (2016).
18. Kong, L, Cui, M: In vivo fluorescence microscopy via iterative multi-photon adaptive compensation technique. Opt. Express 22, 23786-23794 (2014).